Assessment of Geohazards along Highways Based on the Weights of Evidence and GIS: A Case Study in Guangxi Province, China

Yue Zhao
Chang'an University
Hongzhi Yang (yhz@chd.edu.cn)
Chang'an University https://orcid.org/0000-0001-6152-8739
Lixiang Yin
Chang'an University
Junnan Li
Chang'an University

Research Article

Keywords: Highway, geohazards, risk assessment, weights of evidence method, intensity index, sensitivity index

Posted Date: March 23rd, 2022

DOI: https://doi.org/10.21203/rs.3.rs-1002401/v1

Title

Assessment of Geohazards along Highways Based on the Weights of Evidence and GIS: A Case Study in Guangxi Province, China

Author Information

Yue Zhao (the first author)
School of Highway, Chang'an University
ORCiD: http://orcid.org/0000-0002-1938-9904
2020121223@chd.edu.cn

Hongzhi Yang (the second author & the corresponding author)
School of Highway, Chang'an University
Middle section of Nan'er Huan Road Xi'an, ShaanXi Province, 710064, China
ORCiD: http://orcid.org/0000-0001-6152-8739
yhz@chd.edu.cn

Lixiang Yin (the third author)
School of Highway, Chang'an University
2020221310@chd.edu.cn

Junnan Li (the fourth author)
School of Highway, Chang'an University
2021221328@chd.edu.cn

Abstract

Geological disasters damage highways and disrupt traffic, which reduces the service level of roads. We collected 15,435 geohazards in Guangxi Province. The geohazards within 1km of the highway buffer were selected to study its spatial distribution characteristics and risk assessment methods. Geohazard intensity index and sensitivity index are proposed to establish the highway geohazards assessment model. Based on the weights of evidence (WOE) method, the influencing factors of the sensitivity index and the weight of each factor are obtained. By analyzing the spatial distribution characteristics of geohazards, collapses, landslides, ground collapse and unstable slopes are identified as major geohazards along the highway. Based on the Getis-Ord Gi* statistic methods, the hotspot map of four disasters was drawn, and the intensity index along the highway was calculated. The relationship between slope, aspect, topographic relief, annual average rainfall, land use, lithology type and geohazards was analyzed.

The sensitivity index was calculated using the WOE method. The intensity index and the sensitivity index were superimposed to obtain the geohazard index, and the geohazard risk of the highway is divided into five levels. The model accuracy-test based on the receiver operating characteristic (ROC) curve shows that Area Under Curve (AUC) equals 0.71, indicating high reliability for the risk assessment.

Keywords

Highway; geohazards; risk assessment; weights of evidence method; intensity index; sensitivity index

Statements and Declaration

This research was funded by Chang'an University (Xi'an, China) through the National Key Research & Development Program of China (2020YFC1512003).
No potential conflict of interest was reported by the author(s).

Assessment of Geohazards along Highways Based on the Weights of Evidence and GIS: A Case Study in Guangxi Province, China

Abstract

Geological disasters damage highways and disrupt traffic, which reduces the service level of roads. We collected 15,435 geohazards in Guangxi Province. The geohazards within 1km of the highway buffer were selected to study its spatial distribution characteristics and risk assessment methods. Geohazard intensity index and sensitivity index are proposed to establish the highway geohazards assessment model. Based on the weights of evidence (WOE) method, the influencing factors of the sensitivity index and the weight of each factor are obtained. By analyzing the spatial distribution characteristics of geohazards, collapses, landslides, ground collapse and unstable slopes are identified as major geohazards along the highway. Based on the Getis-Ord Gi* statistic methods, the hotspot map of four disasters was drawn, and the intensity index along the highway was calculated. The relationship between slope, aspect, topographic relief, annual average rainfall, land use, lithology type and geohazards was analyzed. The sensitivity index was calculated using the WOE method. The intensity index and the sensitivity index were superimposed to obtain the geohazard index, and the geohazard risk of the highway is divided into five levels. The model accuracy-test based on the receiver operating characteristic (ROC) curve shows that Area Under Curve (AUC) equals 0.71, indicating high reliability for the risk assessment.

Keywords: Highway; geohazards; risk assessment; weights of evidence method; hot spot analysis; intensity index; sensitivity index

1 Introduction

In the context of global climate change, the risk of natural hazards facing humanity continues to increase (Church et al. 2013). China is a country with frequent geohazards, and 50% of the arterials are in areas prone to geohazards. Traffic interruptions caused

by geohazards such as landslides, collapses, and debris flow increased from more than 5,800 in 2010 to more than 18,000 in 2019 (Liu et al. 2020). Studying the spatial distribution, influencing factors, and risk assessment methods of geohazards along highways can provide a basis for road network design and emergency traffic management.

Studies on the evaluation of geological hazards along the highway focus on the regional highway geohazard zoning, the risk prediction of geohazards along the highway, and the geological risk evaluation methods.

Regional geohazard zoning is based on the analysis of topography, geology, rainfall and other influencing factors, and the area is divided into different risk areas based on the overlap of weights and various factors. Based on statistical analysis, Xiao et al. (2019) adopted an improved backward cloud algorithm and integrated internal and trigger factors to conduct a risk analysis of Taiwan's highway collapse. J. et al. (2015) conducted a sensitivity analysis on the subsidence of karst areas based on the WOE method. Researchers use logistic regression models (Behnia et al. 2018, Kim et al. 2016), frequency ratio methods (Regmi et al. 2016, Yusof et al. 2015), the analytic hierarchy process (AHP) method (Lyu et al. 2018, Vaani et al. 2012, Zhang, He, et al. 2018), machine learning method (A.H.Al-Najjar et al. 2021, Kai et al. 2018) and other models, and select various influencing factors to classify geological disasters such as landslides and collapses, and determine the prone areas.

The geological risk prediction along highways is to predict the risk level of different sections by analyzing the spatial distribution and influencing factors of geohazards within the highway buffer zones, using statistical and mathematical models (Huang et al. 2018). Based on big data mining, Wen et al. (2018) selected 13 landslide susceptibility factors such as elevation, slope, and lithology to predict the landslide susceptibility along mountain highways. According to the risk zoning of the highway slope disaster in northern Shaanxi, Zhao et al. (2018) selected five factors such as slope, annual precipitation, and vegetation coverage to establish a highway slope risk assessment model. Amatya et al. (2019) took 3km along the road as a buffer zone, and

select factors such as slope, aspect and land cover based on the logistic regression method to divide the sensitivity along the Karnali highway.

The geological risk assessment method includes two aspects: weight determination and model framework. Models framework include supporting entropy method, information method, WOE method and logistic regression model, etc. (Boyu et al. 2020, Du et al. 2016, Guo et al. 2015, Trigila et al. 2015, Vakhshoori et al. 2016, Yusof et al. 2015). The weight determination can be divided into deterministic methods and subjective uncertainty methods. The deterministic method incomplete additive linguistic matrix is applied to determine the weight of each impact factor based on (Yang et al. 2020). Cui et al. (2018) uses the expert scoring method to determine the weights of four types of factors such as the risk of heavy rain disasters and the vulnerability of the carrying body, and builds a heavy rain disaster risk zoning model for Shanghai-Wuhan-Chengdu high-speed railway.

The current studies focus on the risk assessment of geohazards for a single hazard, a certain section of the highway, or the study of the relationship between natural factors and geohazards (Ma 2013). The multi-hazard and multi-factor geohazard assessment research for the road network is relatively lacking (Qiao 2006, Tian et al. 2019). Based on the geohazard data along the highway in Guangxi, this paper studies the distribution characteristics and influencing factors of various geohazards. Based on the WOE method, the geohazard intensity index and sensitivity index are calculated, and the Guangxi road network's geohazard risk classification map is obtained, which provides a basis for road network hazard prevention and control.

2 Study area

The study area is Shandong Province located in south China (20°54 ' to 26°24'N and 104°28 ' to 112°04'E). The landform is mountainous and hilly, and karst is the main feature. Guangxi has a subtropical and tropical monsoon climate with abundant rainfall and an average annual rainfall of about 1800mm.

The types and distribution of geohazards are closely related to regional geological conditions and environmental conditions. Guangxi is a typical mountainous and hilly

area. Collapse and landslide are the two most common geohazards (Peng et al. 2015). The total number of geohazards in the study area is 15,435, of which collapse accounted for 48.6%, landslide accounted for 27.4%, ground collapse accounted for 13.1%, unstable slope accounted for 8.5%, ground fissure accounted for 1.5%, and debris flow accounted for 0.9%. The total number of geohazards in the 1km highway buffer zone is 3303, accounting for 21.4% of the total. Fig 1 shows the distribution of geohazards along the highway in Guangxi Province.

The number of geohazards of debris flow in the buffer is 22, only 0.7% of the total. Therefore, the debris flow is not considered for geohazard risk assessment. Table 1 lists the types and sources of data used in the research.

Data used in the article include road network, topography, rainfall, geology, etc. These data come from different institutions and field surveys. Using GIS tools, we carried out projection transformation and calibrated the data. Table 1 lists the type and data sources.

3 Methodology

By revealing the relationship between historical geohazards and environmental factors along highways in Guangxi Province, this paper analyzes the intensity and sensitivity of multi-hazard geohazards suffered by highway infrastructure and makes an evaluation. Fig 2 is the methodology diagram for analyzing multi-hazard geohazards along highways based on the WOE method.

3.1 Geohazard assessment indicators

The geohazard assessment model along the highway should reflect the current development of geohazards and evaluate the possibility of geohazards in the future. Therefore, the geohazard risk index includes two parts: intensity index and sensitivity index. The intensity index is calculated by analyzing the spatial characteristics of geohazards along the highway. The sensitivity index analyzes the environmental factors related to geohazards and then superimposes calculations to reflect the possibility of geohazards' risk. Thus, the geohazard risk index is obtained by superimposing the intensity index and the sensitivity index. The calculation formula can be expressed as:

$$C_i = T_i W_t + S_i W_s \quad (1)$$

where, C_i is the i^{th} grid multi-hazard geohazard risk index along the highway; T_i is the value of the geohazard intensity index in i^{th} grid, and S_i is the value of the geohazard sensitivity index in i^{th} grid; W_t and W_s are the weights of the intensity index and the sensitivity index, respectively.

The geohazard intensity index reflects the damage to the highway by the multi-hazard geohazards in the geographic unit (Shang et al. 2005). The geohazard intensity index along the highway in Guangxi is mainly determined by four geohazards: collapse, landslide, ground collapse, and unstable slope. The calculation of the intensity index of multi-hazard geohazards along the highway in Guangxi is shown in formula (2):

$$T_i = \sum_{j=1}^{N} Q_{ij} W_j^Q \tag{2}$$

where, Q_{ij} is the intensity index score of the j^{th} geological hazard in the i^{th} grid, and W_j^Q is the weight of the j^{th} geological hazard.

The geohazard sensitivity index reflects the relationship between the various influencing factors in the geographic unit and geohazards (Behnia et al. 2018). This paper selects six influencing factors such as slope to determine the sensitivity index of geohazards along the Guangxi highway. The calculation method is expressed in formula (3):

$$S_i = \sum_{j=1}^{N} P_{ij} W_j^P \tag{3}$$

where, P_{ij} is the intensity index score of the j^{th} impact factor in the i^{th} grid, and W_j^P is the weight of the j^{th} impact factor.

3.2 Weights of evidence method

WOE method is a geological statistical method proposed by Canadian mathematical geologist Agterberg (Carranza 2004). The principles of WOE in geohazard risk analysis are as follows.

The study area is divided into equal-area N[T] evaluation units. Definition D means that geohazards have occurred, the number of units with geohazards in the study area

188 is N[D], and the number of units without geohazards is $\mathrm{N}[\overline{D}]$, which can be calculated:

189 $$\mathrm{N}[\overline{D}] = \mathrm{N}[\mathrm{T}] - \mathrm{N}[\mathrm{D}] \quad (4)$$

190 The prior probability of geohazards in any unit is:

191 $$P_{prior} = P[D] = \frac{\mathrm{N}[\mathrm{D}]}{\mathrm{N}[\mathrm{T}]} \quad (5)$$

192 Define the evidence factor related to the geohazard as B, then the j^{th} evidence layer
193 can be expressed as $\{B_j\}$, the number of units with the evidence factor in the study area
194 is $\mathrm{N}[B_j]$, and the number of units without the evidence factor is $\mathrm{N}[B_j]$, the
195 corresponding positive weight W_j^+ and negative weight W_j^- are calculated as
196 follows:

197 $$W_j^+ = \ln\frac{P\{B_j|D\}}{P\{B_j|\overline{D}\}} = \ln\frac{\frac{N\{B_j \cap D\}}{\mathrm{N}[\mathrm{D}]}}{\frac{N\{B_j \cap \overline{D}\}}{\mathrm{N}[\overline{D}]}} \quad (6)$$

198 $$W_j^- = \ln\frac{P\{\overline{B}_j|D\}}{P\{\overline{B}_j|\overline{D}\}} = \ln\frac{\frac{N\{\overline{B}_j \cap D\}}{\mathrm{N}[\mathrm{D}]}}{\frac{N\{\overline{B}_j \cap \overline{D}\}}{\mathrm{N}[\overline{D}]}} \quad (7)$$

199 Where, $\mathrm{N}\{B_j \cap D\}$ represents the number of units that contain both evidence layers
200 $\{B_j\}$ and geohazards, $N\{B_j \cap \overline{D}\}$ represents the number of units that contain evidence
201 layers $\{B_j\}$ without geohazards, $N\{\overline{B}_j \cap \overline{D}\}$ represents the number of units that do not
202 contain the evidence layer $\{B_j\}$ and geohazards occur, and $N\{\overline{B}_j \cap \overline{D}\}$ represents the
203 number of units that neither contains the evidence layer $\{B_j\}$ nor have geohazards
204 occurred.

205 When $W_j^+ > 0$ or $W_j^- < 0$, it means that the evidence factor is positively correlated
206 with geohazards, when $W_j^+ < 0$ or $W_j^- > 0$, the evidence factor is negatively
207 correlated with geohazards, when $W_j^+ = 0$ or $W_j^- = 0$, the evidence factor is not
208 related to geohazards. The C value represents the comprehensive weight, that is, the

weights of the evidence layer's influence on the occurrence of geohazards (Fan et al. 2015, Hu et al. 2020, Xiao 2013). The calculation is shown in the following formula.

$$C = W_j^+ - W_j^- \tag{8}$$

The WOE method assumes that the evidence factors are conditionally independent, and the independence test of the evidence factors is required (Sun et al. 2019). In order to simplify the calculation, the symbol $O\{D\}$ is introduced, which is defined as the prior probability $O\{D\}$, then:

$$\ln\left[O\{D\middle|B_1^k \cap B_2^k \cap \cdots \cap B_n^k\}\right] = \ln[O\{D\}] + \sum_{j=1}^{n} W_j^k \tag{9}$$

where, n is the number of evidence layers, k is the existing status of the evidence layers, W_j^k calculated for the existence of k is W_j^+, if the evidence does not exist, W_j^-, if the data is missing, then $W_j^k = 0$.

3.3 Hot spot analysis

Based on the classified and weighted geohazards, this paper uses the ArcGIS hotspot tool to analyze the intensity of geohazards along the highway in Guangxi. The hot spot analysis calculates Getis-Ord Gi* statistics for each element in the data set, and obtains the z-score and p-value, so that the spatial concentration positions of high-value and low-value elements are obtained (Shen et al. 2021). The local statistics of Getis-Ord can be expressed as:

$$G_i^* = \frac{\sum_{j=1}^{n} w_{i,j}x_j - \bar{X}\sum_{j=1}^{n} w_{i,j}}{S\sqrt{\frac{\left[n\sum_{j=1}^{n} w_{i,j}^2 - \left(\sum_{j=1}^{n} w_{i,j}\right)^2\right]}{n-1}}} \tag{11}$$

where, x_j is the attribute value of element j, $w_{i,j}$ is the spatial weight between elements i and j, n is the total number of elements, and:

$$\bar{X} = \frac{\sum_{j=1}^{n} x_j}{n} \tag{12}$$

$$\mathrm{S} = \sqrt{\frac{\sum_{j=1}^{n} x_j^2}{n} - (\bar{X})^2} \tag{13}$$

The Gi* statistic returned for each element in the data set is the z-score. For a

statistically significant positive z-score, the higher the z-score, the tighter the clusters of high values (hot spots). For statistically significant negative z-scores, the lower the z-score, the tighter the clustering of low values (cold spots).

3.4 Receiver operating characteristic curve

ROC curve, also known as sensitivity curve, was initially used in the military and then widely used in medical diagnosis. The most intuitive application of ROC is to reflect model sensitivity (FPF) and specificity (TPF), so it is also widely used in the assessment of geohazard susceptibility (Quanfu et al. 2017).

Based on the confusion matrix shown in Table 2, the calculation formula of ROC's False Positive Fraction (FPF) on the abscissa and True Positive Fraction (TPF) on the ordinate is as follows.

$$\mathrm{FPF} = \frac{FP}{TN + FP} \tag{14}$$

$$\mathrm{TPF} = \frac{TP}{TP + FN} \tag{15}$$

AUC is defined as the area under the ROC curve to reflect the model's accuracy intuitively, and its value is generally between 0.5-1 (Yang et al. 2021). When AUC=0.5, just like random guessing, the model has no predictive value. When 0.5<AUC<1, model prediction is better than random prediction and has predictive value.

4 Geohazard Intensity Index

Geohazard intensity index reflects the spatial characteristics of geohazards (Yang et al.). The density and intensity of geohazards reflect the degree of geological risk in a specific highway section. The Getis-Ord Gi* statistic method can effectively identify statistically significant hotspots and is used for geohazards intensity analysis. This paper uses the Getis-Ord Gi* statistic method to calculate the z-score of collapses, landslides, ground collapses and unstable slopes, and draws the hot spot analysis map. For hot spot analysis, it is necessary to classify geological disasters by intensity. As shown in Table 3, according to China's geohazard classification system, geohazards can be divided into four levels: minor, medium, large, and extra-large hazard. Based on the classification of geohazards, the GIS platform is used to analyze the hot spots of various

geohazards in the buffer zone and obtain the intensity index of different geohazards on the road network, as shown in Fig 3.

The multi-hazard intensity index of geohazards in the buffer zone is a weighted superposition of the hotspot analysis of individual geohazards. The weights are determined by expert scoring. We invited 15 geohazard experts, 11 highway experts and 6 traffic safety experts, and 28 valid questionnaires were recovered. This survey determined the degree of damage caused by different geohazards to the highway, and the weights are shown in Table 4. The multi-hazard intensity index is obtained by GIS weighted superposition according to the hazard weight, as shown in Fig 4.

From the intensity index, we can get the following conclusions about the spatial distribution of geohazards along the highway in Guangxi:

1. The geohazards along the highway in Guangxi mainly collapses, accounting for 45% of the total geohazards. The risk levels of geohazards along the highway are divided into four levels: minor, medium, large and extra-large according to the degree and scale of geohazards. Minor geohazards accounted for 71.5%.
2. The hot spots of geohazards along highways are concentrated in mountainous and hilly areas, while the distribution of geohazards in the Guangxi Basin is relatively small. Collapses and landslides are mainly distributed in mountainous areas with steep slopes around the basin. The ground collapse is widespread in the northeastern. The areas with prominent development of unstable slopes are concentrated in the northeast and southeast.

5 Geohazard Sensitivity Index

The geohazard sensitivity index reflects the relationship between the natural environment and geohazards (Quancheng et al. 2015, Yang et al. 2020). Variables related to environmental characteristics and geohazards can be divided into four categories: meteorological, surface, geological, and hydrological.

5.1 Impact factor

This paper selects average annual rainfall, lithology type, land use, slope, aspect and topographic relief to calculate the sensitivity index and reflect the possibility of

geohazards.

Average Annual Rainfall

Rainfall is one of the direct factors that induce geohazards (Chen et al. 2016, Zhang, Zhao, et al. 2018). Precipitation-induced geohazards have the characteristics of group-occurring, simultaneity, sudden breakout, and serious consequences (Li 2005).

Fig 5 is the distribution map of the average annual rainfall over the 20 years (1999-2019) in the study area. Fig 6 shows the relationship between the average annual rainfall and the frequency of geohazards. Geohazards mainly occur in areas with an average annual rainfall of 1600mm-1800mm, accounting for 60.5% of the total. The distribution density of geohazards is the highest, where the average annual rainfall is greater than 1700mm.

Lithology Type

The lithology types in the study area can be divided into hard rock, medium rock, soft rock, and soft and hard rocks alternate-layered, as shown in Fig 7. The relationship between lithology and the frequency of geological disasters is shown in Fig 8. Geohazards mainly occur on hard rock, accounting for about 50%, followed by medium rock and soft and hard rocks alternate-layered.

Land Use

The vegetation coverage in the study area is very high, and the relationship between geological disasters and vegetation coverage is not obvious. From the relationship between land use types and geohazards in Figs 9 and 10, it can be seen that the relationship between the two is apparent. More than half of the geohazards occurred in forest land, followed by agricultural land. In mountainous forest land, the disturbance of highway construction increases the risk of geohazards.

Slope

The slope is one of the main factors affecting geohazards. Based on DEM, the slope distribution of the study area can be obtained. After reclassifying the results, the slope distribution is shown in Fig 11. From Fig 12, geohazards mainly occur in the Guangxi Basin, where the slope is less than 3%. When the slope is greater than 10%, the

geohazards are the least. The reason is that the design of Guangxi highway often bypasses steep slopes or uses tunnels.

Aspect

The aspect is one of the essential factors affecting the intensity of the mountain surface sunshine and solar radiation. It is related to mountain ecology and surface morphology, and affects geohazards to a certain extent. Fig 13 and Fig 14 show the relationship between aspect and geohazards.

Topographic Relief

Topographic relief is a quantitative indicator to describe the morphology of landforms. Using the spatial analysis function of ArcGIS, the topographic relief of the study area can be extracted based on DEM, and the natural discontinuity method can be used to reclassify it, as shown in Fig 15. As shown in Fig 16, geohazards mainly occur in the range of topographic relief of 0-63.6, and the number of geohazards shows a decreasing trend with the increase of topographic relief. This trend is related to avoiding areas with complex terrain as much as possible in highway design.

5.2 Sensitivity index calculation

After determining the environmental factors affecting geological disasters, the sensitivity index can be calculated. The study area is divided into $100\text{m} \times 100\text{m}$ grid units (N[T]=23745736), of which 15197 grids have hazard points, that is, N[D]=15197. The prior probability of geological hazards is: $P_{prior} = \frac{15197}{23745736} = 6.4 \times 10^{-4}$.

The weights and contrasts of the evidence factors of each evidence layer are shown in Table 5.

After calculating the weight of each evidence layer, each evidence layer is binarized and the conditional independence test is performed based on the chi-square (χ^2) test. The calculation results are shown in Table 6.

Table 6 shows that all evidence factors meet the conditional independence test. The geohazard sensitivity index along the highway is obtained after normalization of each evidence layer and weighted superposition, as shown in Fig 17. In the figure, when the value is greater than 2.75, the density of geological disasters is the highest. The index

in the eastern region of Guangxi is larger than that in the western region. The reason is that the eastern region has more precipitation, mainly hard rock and medium hard rock.

6 Risk of Multi-hazard Geohazards along Highways

Determining the risk index of geohazards along the highway is significant for highway management, maintenance, and emergency rescue in hazard situations. According to expert scores, the intensity index and sensitivity index weights are 0.41 and 0.59, respectively. The geohazard risk along the highway is obtained by overlapping these two indexes, as shown in Fig 18. The risk index along the highway is divided into 5 levels, where 1 represents the lowest risk, and 5 represents the highest risk.

The ROC curve is used to test the accuracy and sensitivity of the model, as shown in Fig 19. The AUC of the geohazard risk index model is calculated as 0.71. It means the success rate of predicting geohazards along the highway using the model in this paper is 0.71.

From Fig 19, there are the following conclusions:

1. The geohazards risk of highways in the east and southwest of Guangxi Province is relatively high. The east is related to high rainfall, while the southwest is related to the hard rock lithology and the greater disturbance of the ground surface caused by highway construction.
2. The road network in Guangxi Province has many sections with medium and high risks. On the one hand, Guangxi has heavy rainfall and complex terrain, and on the other hand, road construction has a greater disturbance to the ground.
3. When building a highway in areas with high risks, geological disasters should be avoided, and bridges and tunnels should be constructed as far as possible to reduce the occurrence of geohazards.

7 Summary and Conclusion

This paper proposes a highway geohazards risk model with a superimposed intensity index and sensitivity index to provide a basis for highway design, construction, and risk management. Based on the statistical analysis of the existing geological disasters in the highway buffer in Guangxi Province, four typical geohazards are identified as

landslides, collapses, ground collapses, and unstable slopes. The geohazard intensity index obtained by superimposing the hot spot maps of geohazards shows that the current geohazards along the highway are mainly minor, accounting for 71.5%. Landslides and collapses have a high proportion and are closely related to the highway disturbance to the ground. Based on the WOE method, the sensitivity index obtained by superimposing slope, aspect, land use, lithology, rainfall and relief can predict the possibility of geohazards. The sensitivity index shows that the value in eastern Guangxi is higher than that in the west, which is related to rainfall and lithology. The risk index indicates that the risk of geohazards on the highways in eastern and southwestern Guangxi is relatively high, and the natural environment is closely related to highway construction. Therefore, when building highways in high-risk areas, bridges and tunnels should be used as much as possible to avoid geological disasters and reduce disturbance to the ground.

This paper uses the ROC curve to verify the geohazard risk model, and AUC=0.71 indicates high prediction accuracy. There are still subjective factors that need to be improved using the expert scoring method to determine the weight. This research takes the macroscopic road network as the object and seldom considers the relationship between the technical indicators of the highway and the geological disasters. Further research should collect more data and establish a more accurate geohazards risk model based on the relationship between geometric characteristics, slope types, geological disasters, and environmental factors to serve the entire life cycle of the highway.

Reference

A.H.Al-Najjar H, Pradhan B. (2021) Spatial landslide susceptibility assessment using machine learning techniques assisted by additional data created with generative adversarial networks. Geoscience Frontiers 12:625-637. http://doi.org/10.1016/J.GSF.2020.09.002

Amatya P, Kirschbaum D, Stanley T. (2019) Use of Very High-Resolution Optical Data for Landslide Mapping and Susceptibility Analysis along the Karnali Highway, Nepal. Remote Sens 11:1-23. http://doi.org/10.3390/rs11192284

Behnia P, Blais-Stevens A. (2018) Landslide susceptibility modelling using the quantitative random forest method along the northern portion of the Yukon Alaska Highway Corridor, Canada. Nat Hazards 90:1407-1426. http://doi.org/10.1007/s11069-017-3104-z

Boyu W, Chong X, Xiangli H, Siyuan MA, Xiaoyi S, Kai L, Zhongjian Z, Zhengfang L. (2020) Hazard Assessment of Co-seismic Landslides Based on Information Value Method: A Case in 2018 M_W6. 6 Hokkaido Earthquake, Japan. Earthquake Research in China 34:64-80. http://doi.org/10.19743/j.cnki.0891-4176.202001001

Carranza EJM. (2004) Weights of Evidence Modeling of Mineral Potential: A Case Study Using Small Number of Prospects, Abra, Philippines. Natural Resources Research 13:173-187. http://doi.org/10.1023/B:NARR.0000046919.87758.f5

Chen X, Pei Z, Wang F. (2016) GIS-based assessment of rainstorm-induced geological hazards risk in Enshi Autonomous Prefecture. Journal of Geo-information Science 18:343-352. http://doi.org/10.3724/SP.J.1047.2016.00343

Church J, Clark P, Cazenave A, Gregory J, Unnikrishnan A. (2013) Climate Change 2013: The Physical Science Basis. Contribution of Working Group I to the Fifth Assessment Report of the Intergovernmental Panel on Climate Change.

Cui X, Fu J, Dai J, Liu J, Zhou X. (2018) GIS-based rainstorm disaster risk zoning over Shanghai-Wuhan-Chengdu high-speed railway. Journal of the Meteorological Sciences 38:113-120. http://doi.org/10.3969/2017jms.0031

Du Y, Peng J, Zhao S, Hu Z, Wang Y. (2016) Ecological risk assessment of landslide disasters in mountainous areas of Southwest China: A case study in Dali Bai Autonomous Prefecture. ACTA GEOGRAPHICA SINICA 71:1544-1561. http://doi.org/10.11821/dlxb201609007

Fan Q, Ju N, Xiang X, Huang J. (2015) Landslides susceptibility assessment using weights of evidence in the Tongzi watershed, China. Journal of Catastrophology 30:124-129. http://doi.org/10.3969/j.issn.1000-811X.2015.01.024

Guo C, Montgomery DR, Zhang Y, Wang K, Yang Z. (2015) Quantitative assessment of landslide susceptibility along the Xianshuihe fault zone, Tibetan Plateau, China. Elsevier 248:93-110. http://doi.org/10.1016/j.geomorph.2015.07.012

Hu Y, Li D, Meng S, Sun Y. (2020) Landslide susceptibility evaluation in Badong County based on weights of evidence method. Bulletin of Geological Science and Technology 39:187-194. http://doi.org/10.19509/j.cnki.dzkq.2020.0320

Huang X, Wang X, Pei J, Xu M, Huang X, Luo Y. (2018) Risk assessment of the areas along the highway due to hazardous material transportation accidents. Nat Hazards

93:1181-1202. http://doi.org/10.1007/s11069-018-3346-4
J. P, C. C, G. N, E. V. (2015) A multicriteria approach to karst subsidence hazard mapping supported by weights-of-evidence analysis. Eng Geol 197:296-305. http://doi.org/10.1016/j.enggeo.2015.09.001
Kai L, Ming W, Yinxue C, Weihua Z, Guiling Y. (2018) Susceptibility of existing and planned Chinese railway system subjected to rainfall-induced multi-hazards. Transportation Research Part A: Policy and Practice 117:214-226. http://doi.org/10.1016/j.tra.2018.08.030
Kim HS, Chung CK, Kim SR, Kim KS. (2016) A GIS-Based Framework for Real-Time Debris-Flow Hazard Assessment for Expressways in Korea. Int J Disaster Risk Sci 7:293-311. http://doi.org/10.1007/s13753-016-0096-3
Li Y. (2005) Method for the Warning of Precipitation-induced Landslides. Dissertation, China University of Geosciences (Beijing)
Liu Y, Ju N, Liu X, Zhang C, Xie M, Zhao W. (2020) Susceptibility Assessment on Influencing Factors of Collapses and Landslides in Guizhou Province. Journal of Catastrophology 35:201-207. http://doi.org/10.3969/j.issn.1000-811X.2020.03.037
Lyu HM, Shen JS, Arulrajah A. (2018) Assessment of Geohazards and Preventative Countermeasures Using AHP Incorporated with GIS in Lanzhou, China. Sustainability 10:1-21. http://doi.org/10.3390/su10020304
Ma J. (2013) GEOLOGICAL HAZARD SUSCEPTIBILITY ASSESSMENT FOR RAILWAY NETWORK IN GUIZHOU PROVINCE. Dissertation, Southwest Jiaotong University
Peng SH, Wang K. (2015) Risk evaluation of geological hazards of mountainous tourist area: a case study of Mengshan, China. Nat Hazards 78:517-529. http://doi.org/10.1007/s11069-015-1724-8
Qiao X. (2006) Research on Risk Assessment of Geological Disasters Along Highways in Complex Mountainous Areas Based on GIS. Dissertation, Chang'an University
Quancheng Y, Chunmei Y, Shanjun L, Feng G. (2015) Correlation analysis of geological hazards and topography in hilly areas in Shandong province. The Chinese Journal of Geological Hazard and Control 26:93-96. http://doi.org/10.16031/j.cnki.issn.1003-8035.2015.02.16
Quanfu N, Feng Z, Zhang Y, Dang X. (2017) Susceptibility Assessment of Disaster Environment for Landslide Hazard based on GIS in Lanzhou Area. Journal of Catastrophology 32:29-35. http://doi.org/10.3969/j.issn.1000-811X.2017.03.006
Regmi AD, Cui P, Dhital MR, Zou Q. (2016) Rock fall hazard and risk assessment along Araniko Highway, Central Nepal Himalaya. Environ Earth Sci 75:1-20. http://doi.org/10.1007/s12665-016-5905-x
Shang YJ, Park HD, Yang ZF. (2005) Engineering geological zonation using interaction matrix of geological factors: An example from one section of Sichuan-Tibet Highway. Geosci J 9:375-387. http://doi.org/10.1007/bf02910326
Shen D, Guo J, Wang Z, Chen J. (2021) Sensitivity assessment of geological hazards based on hot spot analysis and geographic detectors. Environmental Ecology 3:83-89. http://doi.org/CNKI:SUN:HJSX.0.2021-04-017
Sun L, Ren N, Li Y, Hu L. (2019) Risk assessment on karst collapse of the highway subgrade based on weights of evidence method. The Chinese Journal of Geological

Hazard and Control 30:94-100. http://doi.org/10.16031/j.cnki.issn.1003-8035.2019.03.15
Tian S, Tang Q, Zhang S, Han P, Fan X. (2019) Vulnerability Evaluation of Highway Geological Diasters on the Upper Stream of Min River Based on Road Network Structure. HIGHWAY 64:203-208.
Trigila A, Iadanza C, Esposito C, Scarascia-Mugnozza G. (2015) Comparison of Logistic Regression and Random Forests techniques for shallow landslide susceptibility assessment in Giampilieri (NE Sicily, Italy). Elsevier 249:119-136. http://doi.org/10.1016/j.geomorph.2015.06.001
Vaani N, Sekar SK. (2012) Regional Landslide Hazard Zonation and Vulnerability Analysis using AHP and GIS - A Case study of Nilgiris District, Tamil Nadu, India. Disaster Adv 5:171-176. http://doi.org/10.1111/j.1752-1688.2012.00669.x
Vakhshoori V, Zare M. (2016) Landslide susceptibility mapping by comparing weight of evidence, fuzzy logic, and frequency ratio methods. Geomat Nat Hazards Risk 7:1-22. http://doi.org/info:doi/10.1080/19475705.2016.1144655
Wen H, Li Y, Xue J, Xie P. (2018) Landslides susceptibility microzoning along highway in mountainous region based on mining the big data. Journal of Natural Disasters 27:159-165. http://doi.org/10.13577/j.jnd.2018.0421
Xiao J. (2013) A Research in the Application of the Weights of Evidence Method in the Risk Analysis of Karst Collapse. Dissertation, South China University of Technology
Xiao W, Tian W-P. (2019) Hazard assessment and zoning of collapse along highways in China based on backward cloud algorithm. Geomat Nat Hazards Risk 10:1227-1241. http://doi.org/10.1080/19475705.2018.1502691
Yang H, Zhao Y, Cheng Q. (2020) Geohazards regionalization along highways in Shandong Province, China. Geomatics, Natural Hazards & Risk 11:1760-1781. http://doi.org/10.1080/19475705.2020.1810139
Yang S, Li D, Yan L, Huang Y, Wang M. (2021) Landslides Susceptibility Assessment in High and Steep Bank Slopes along Wujiang River Based on Random Forest Model. Safety and Environmental Engineering 28:131-138. http://doi.org/10.13578/j.cnki.issn.1671-1556.20200956
Yusof NM, Pradhan B, Shafri HZM, Jebur MN, Yusoff Z. (2015) Spatial landslide hazard assessment along the Jelapang Corridor of the North-South Expressway in Malaysia using high resolution airborne LiDAR data. Arab J Geosci 8:9789-9800. http://doi.org/10.1007/s12517-015-1937-x
Zhang J, He P, Xiao J, Xu F. (2018) Risk assessment model of expansive soil slope stability based on Fuzzy-AHP method and its engineering application. Geomat Nat Hazards Risk 9:389-402. http://doi.org/10.1080/19475705.2018.1445664
Zhang S, Zhao L, Delgado-Tellez R, Bao H. (2018) A physics-based probabilistic forecasting model for rainfall-induced shallow landslides at regional scale. Natural Hazards and Earth System Sciences 18:969–982. http://doi.org/10.5194/nhess-2016-348
Zhao H, Tian WP, Li JC, Ma BC. (2018) Hazard zoning of trunk highway slope disasters: a case study in northern Shaanxi, China. Bull Eng Geol Environ 77:1355-

529 1364. http://doi.org/10.1007/s10064-017-1178-1
530

Figure Captions

Fig 1. Distribution of geohazards points in the buffer zone

Fig 2. Methodology diagram

Fig 3. Hot spot analysis of geohazards (a) collapses (b) landslides (c) ground collapses (d) unstable slopes

Fig 4. Map of comprehensive intensity index along highways in Guangxi

Fig 5. 20-year average annual rainfall distribution map

Fig 6. Relationship between average annual rainfall and geohazards

Fig 7. Lithology type distribution map

Fig 8. Relationship between lithology type and geohazards

Fig 9. Land use distribution map

Fig 10. Relationship between land use and geohazards

Fig 11. Slope distribution map

Fig 12. Relationship between slope and geohazards

Fig 13. Aspect distribution map

Fig 14. Relationship between aspect and geohazards

Fig 15. Topographic relief distribution map

Fig 16. Relationship between topographic relief and geohazards

Fig 17. Map of geohazard sensitivity index along highways in Guangxi

Fig 18. Geological hazard risk zoning map along highways in Guangxi Province

Fig 19. Map of receiver operating characteristic

Figures

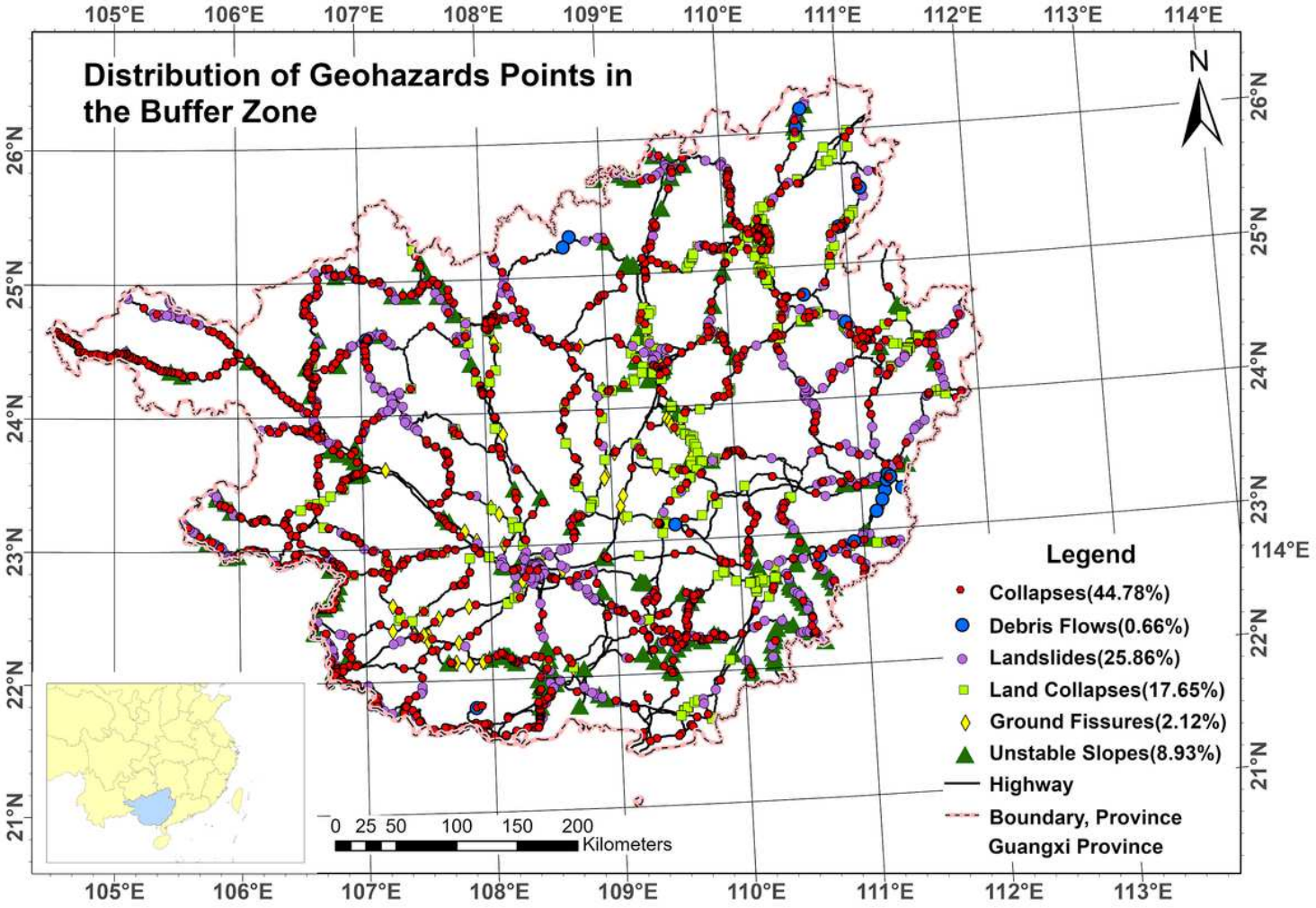

Figure 1

Distribution of geohazards points in the buffer zone

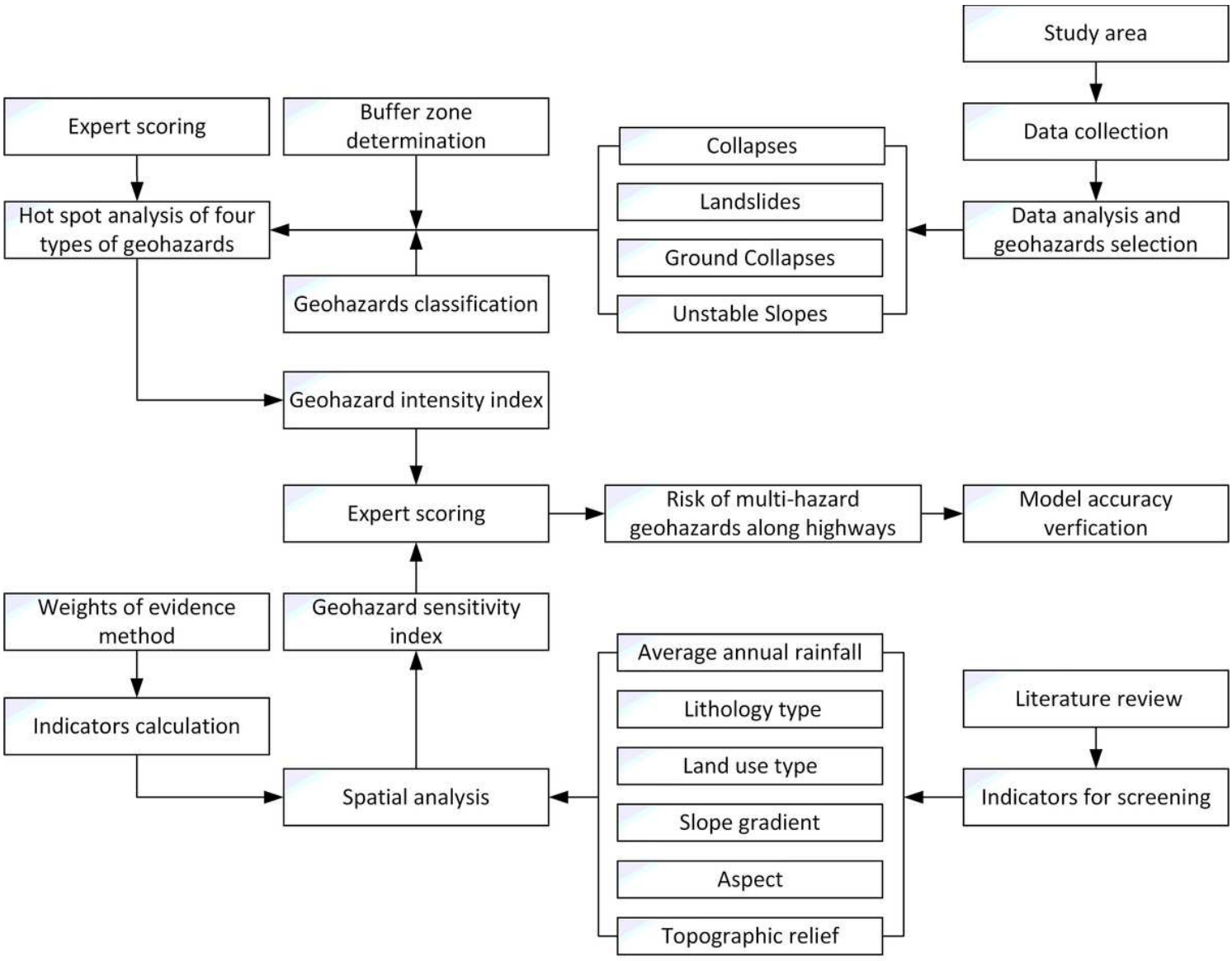

Figure 2

Methodology diagram

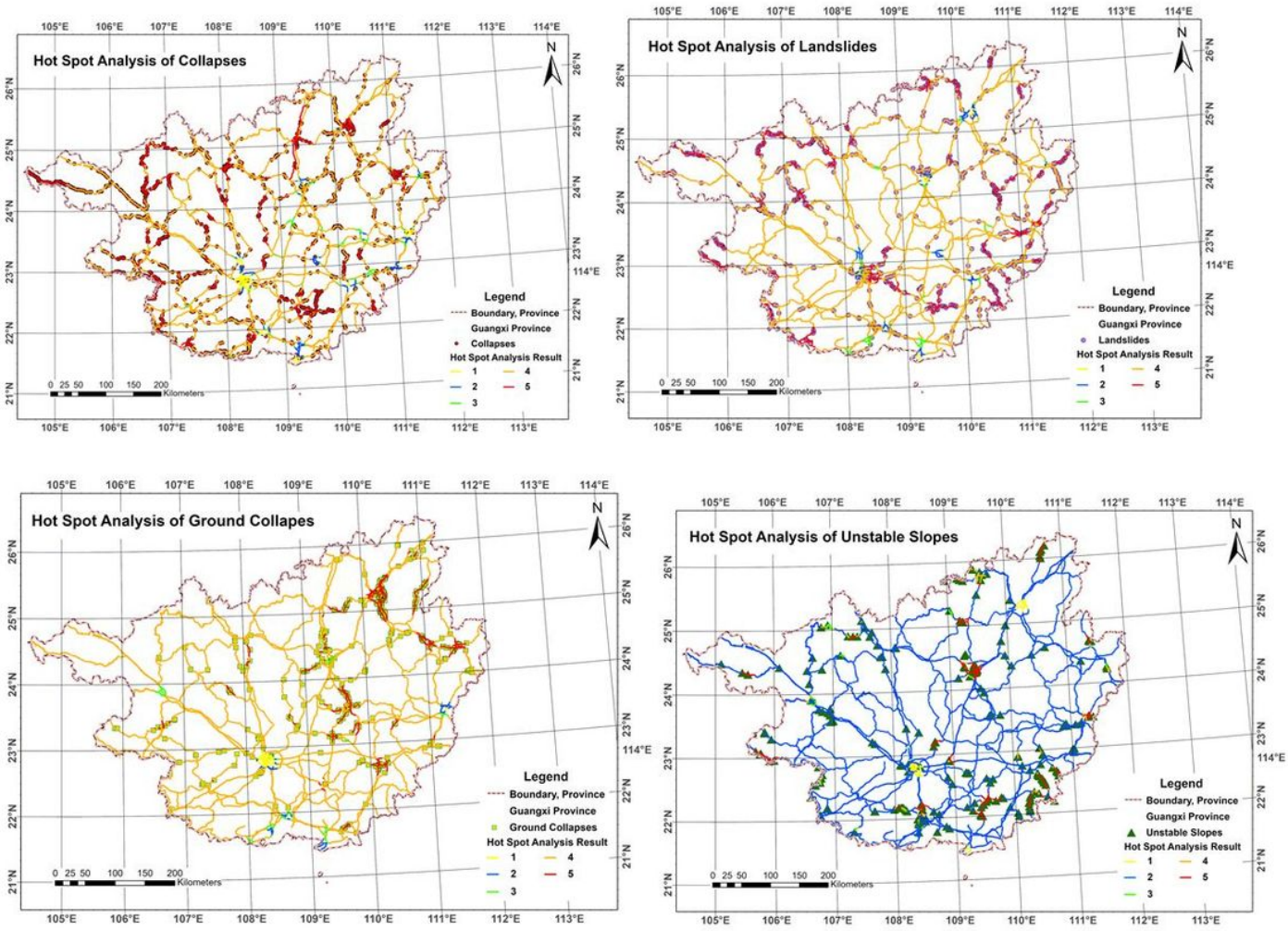

Figure 3

Hot spot analysis of geohazards (a) collapses (b) landslides (c) ground collapses (d) unstable slopes

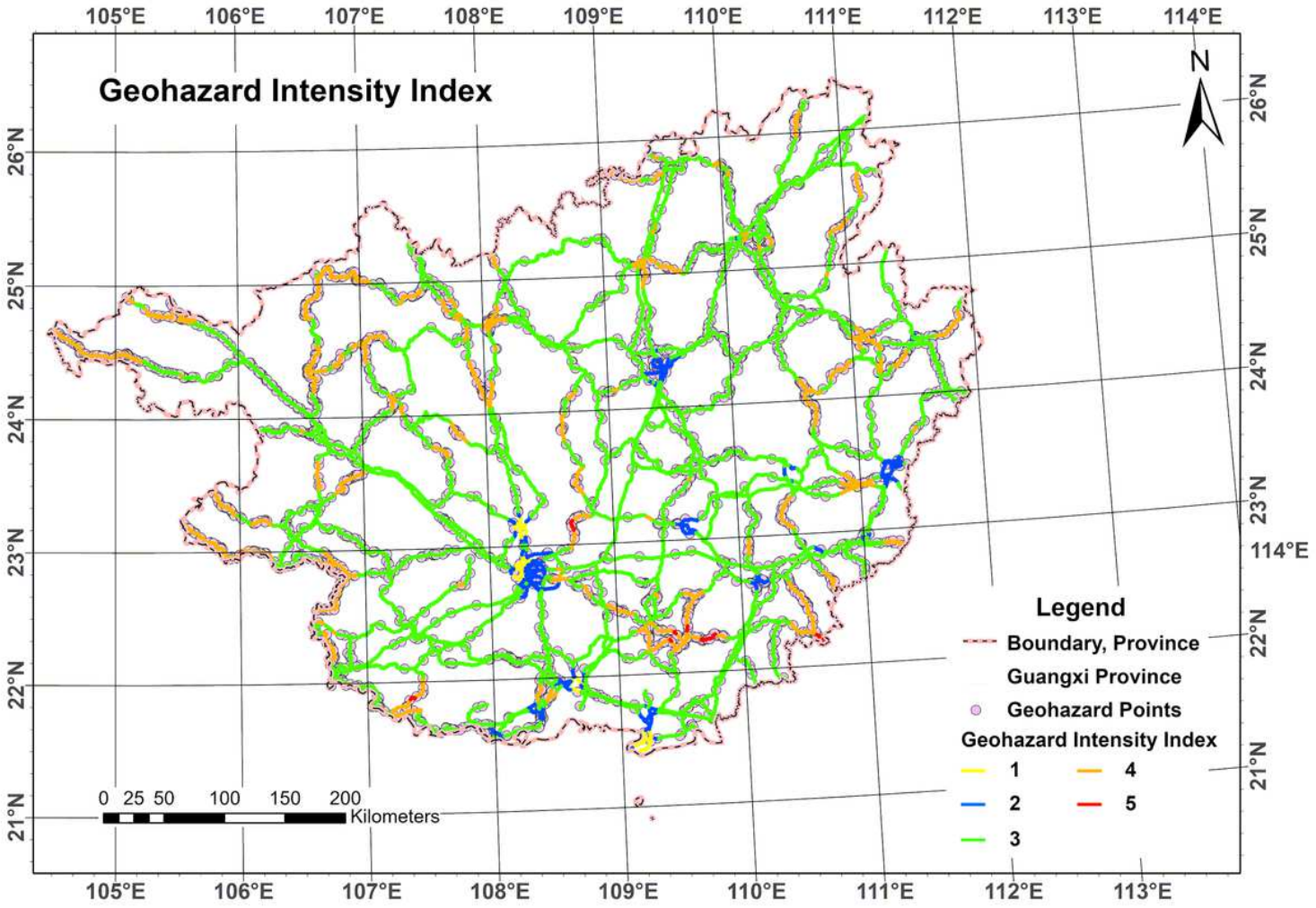

Figure 4

Map of comprehensive intensity index along highways in Guangxi

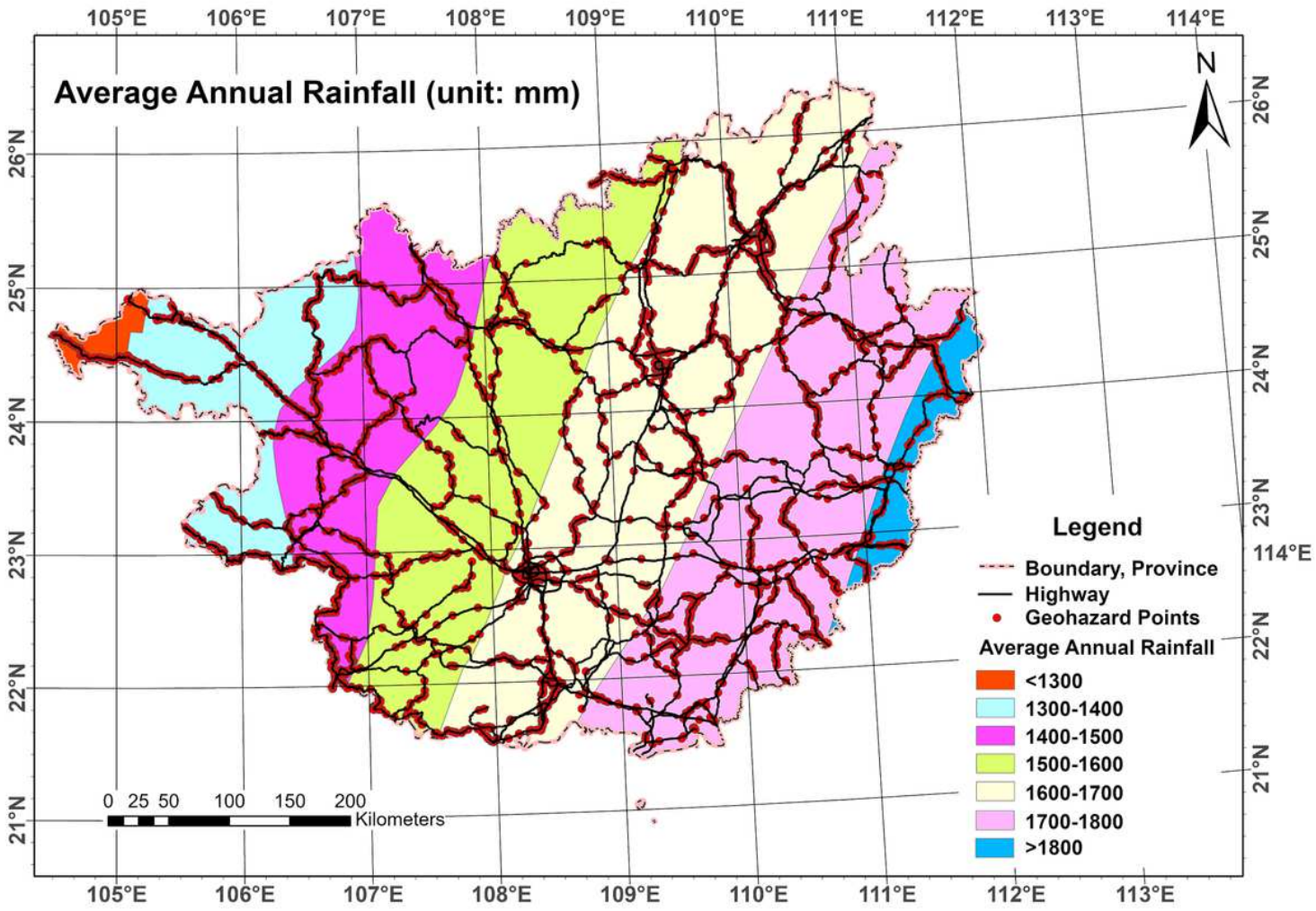

Figure 5

20-year average annual rainfall distribution map

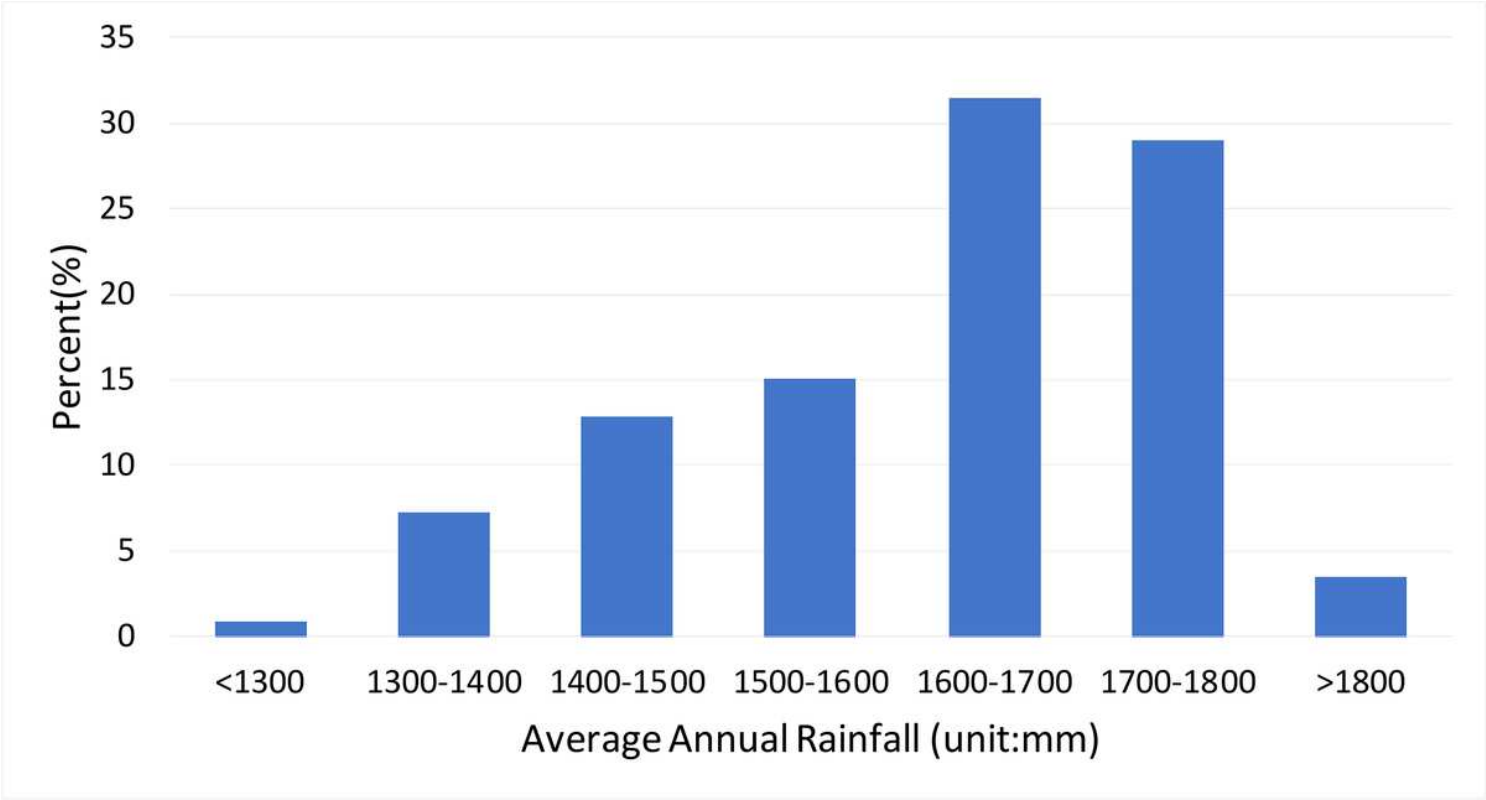

Figure 6

Relationship between average annual rainfall and geohazards

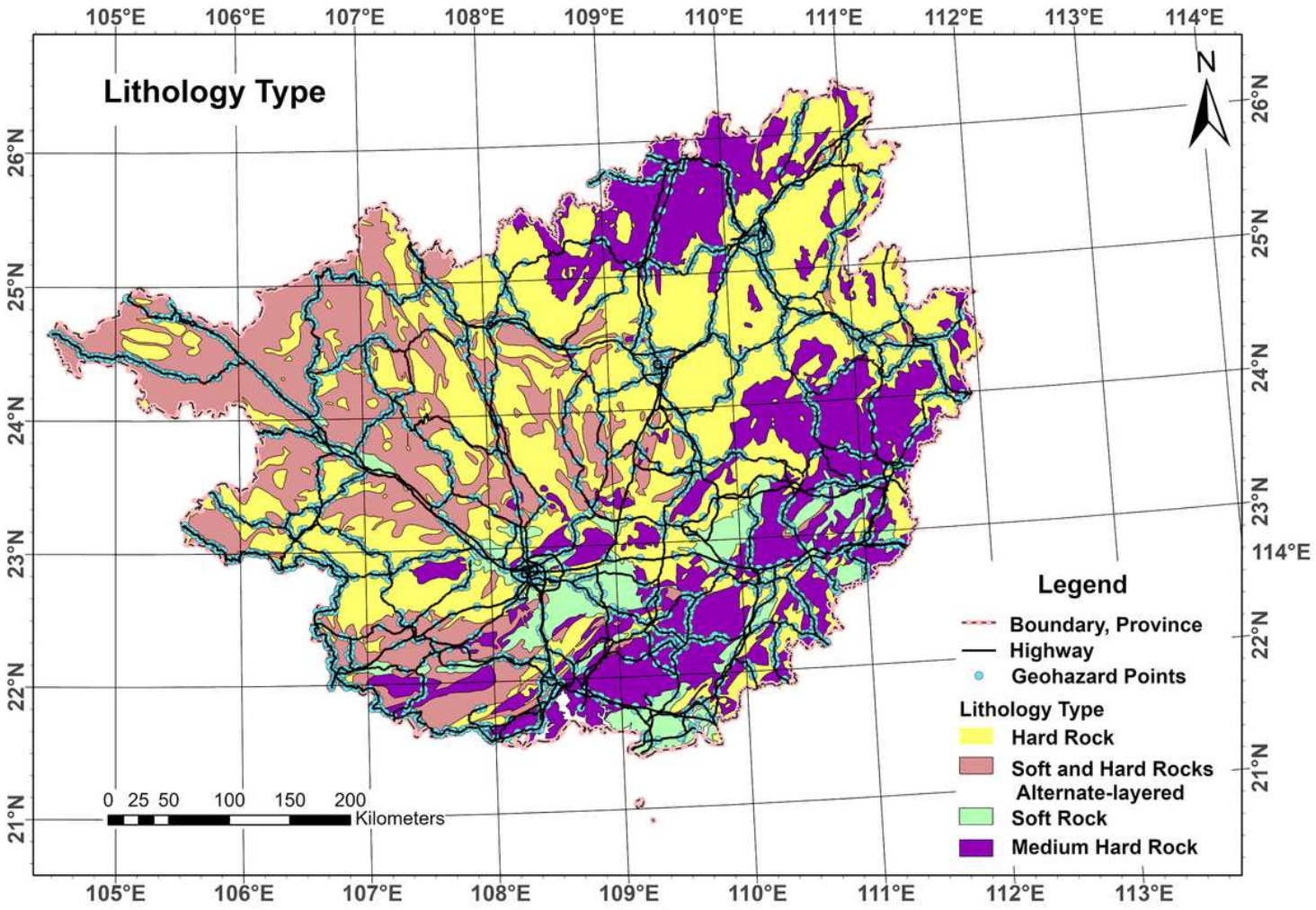

Figure 7

Lithology type distribution map

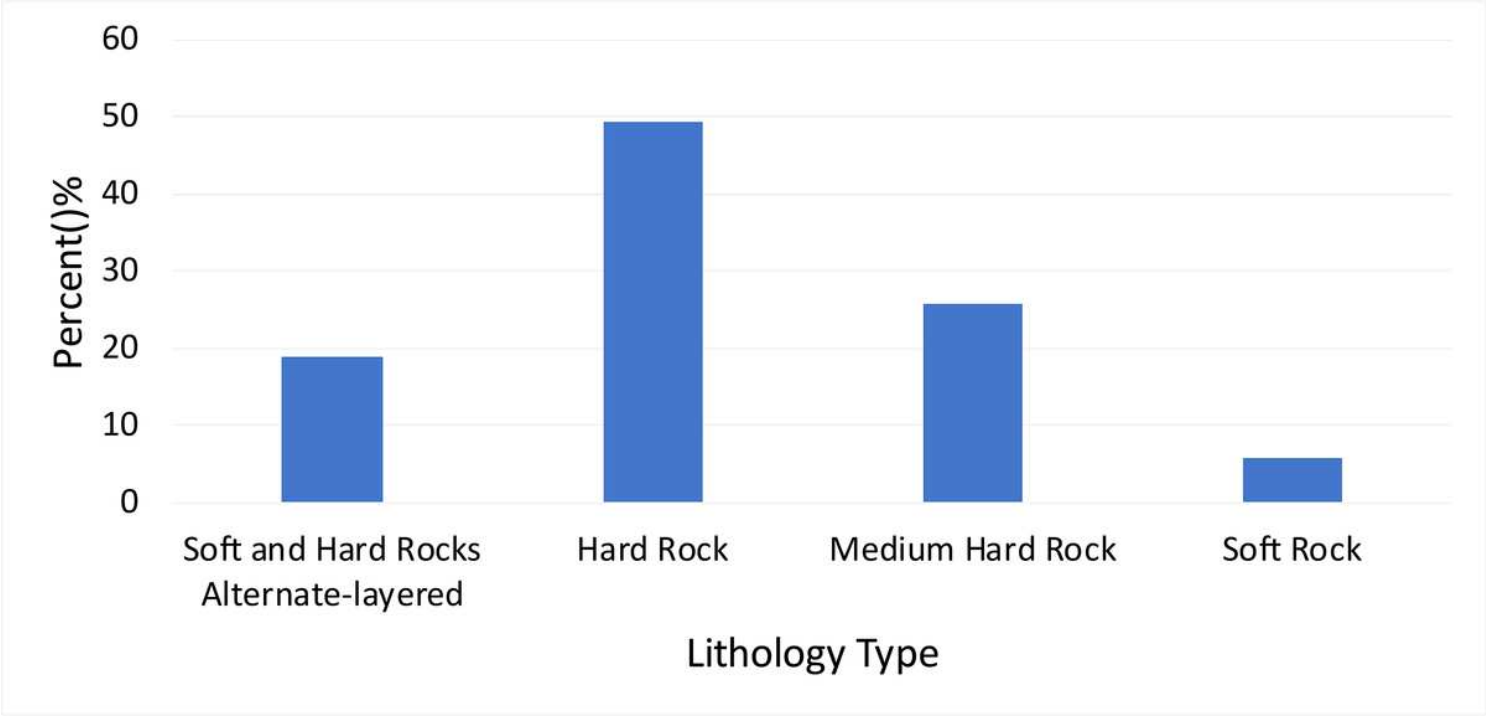

Figure 8

Relationship between lithology type and geohazards

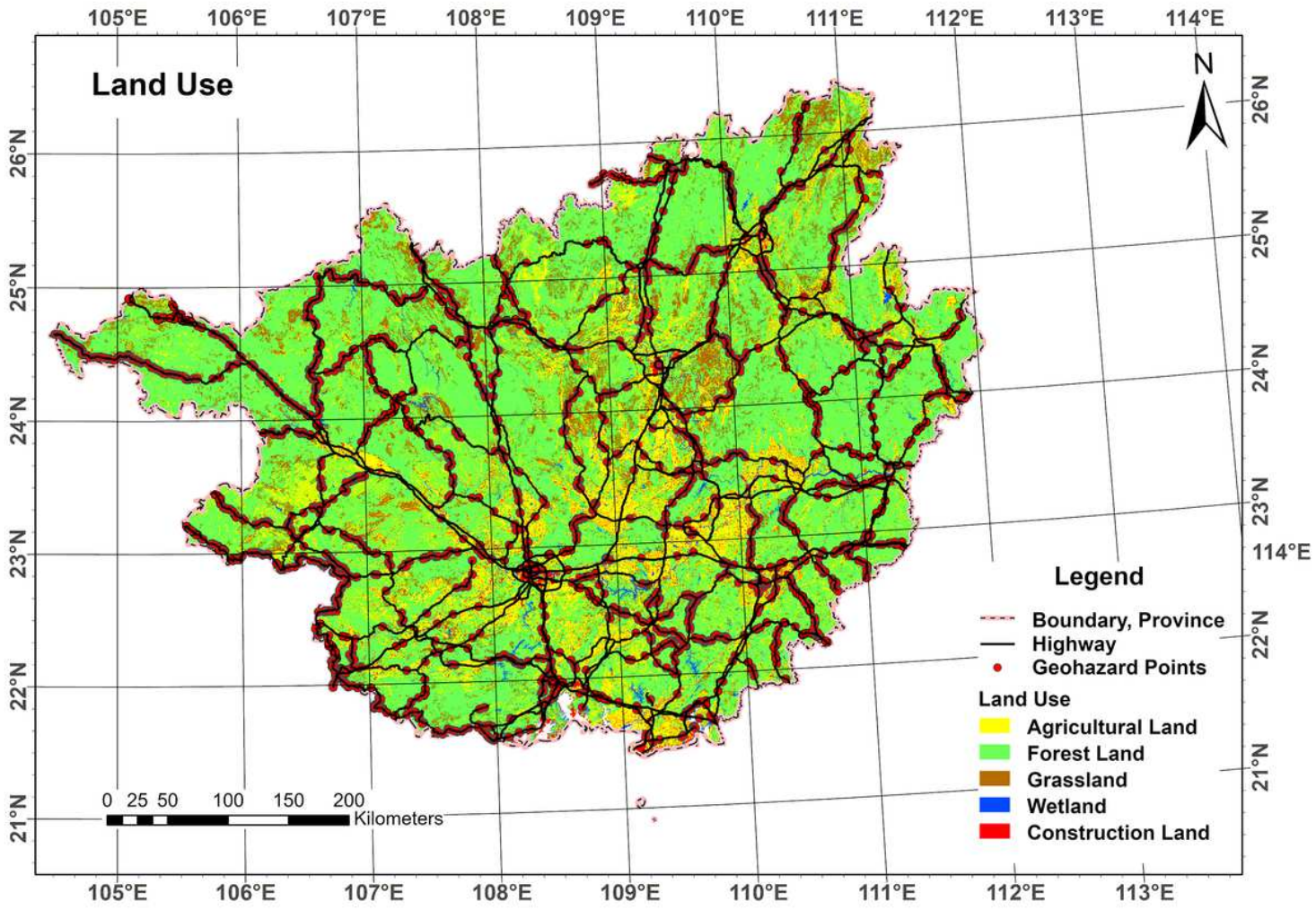

Figure 9

Land use distribution map

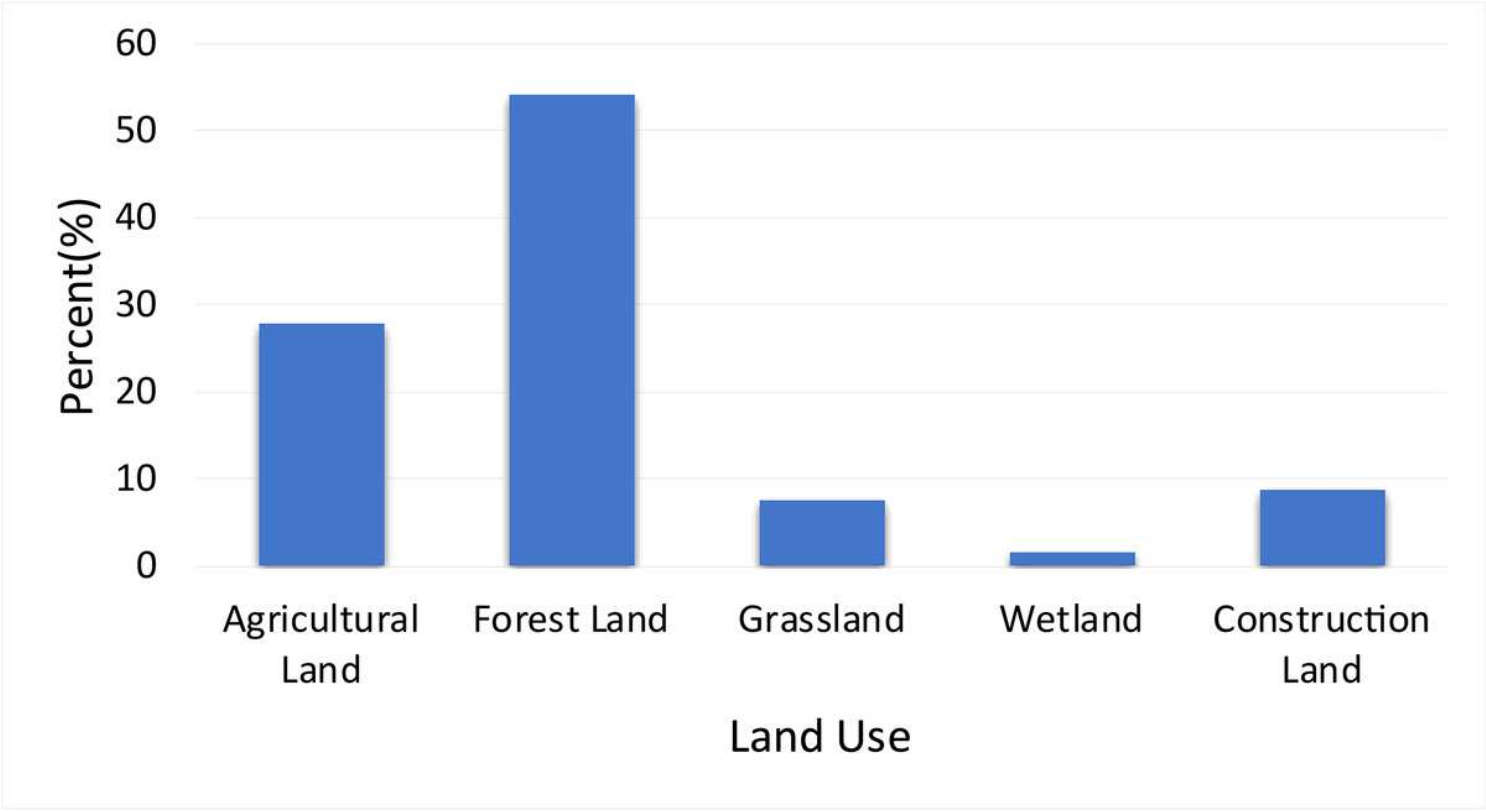

Figure 10

Relationship between land use and geohazards

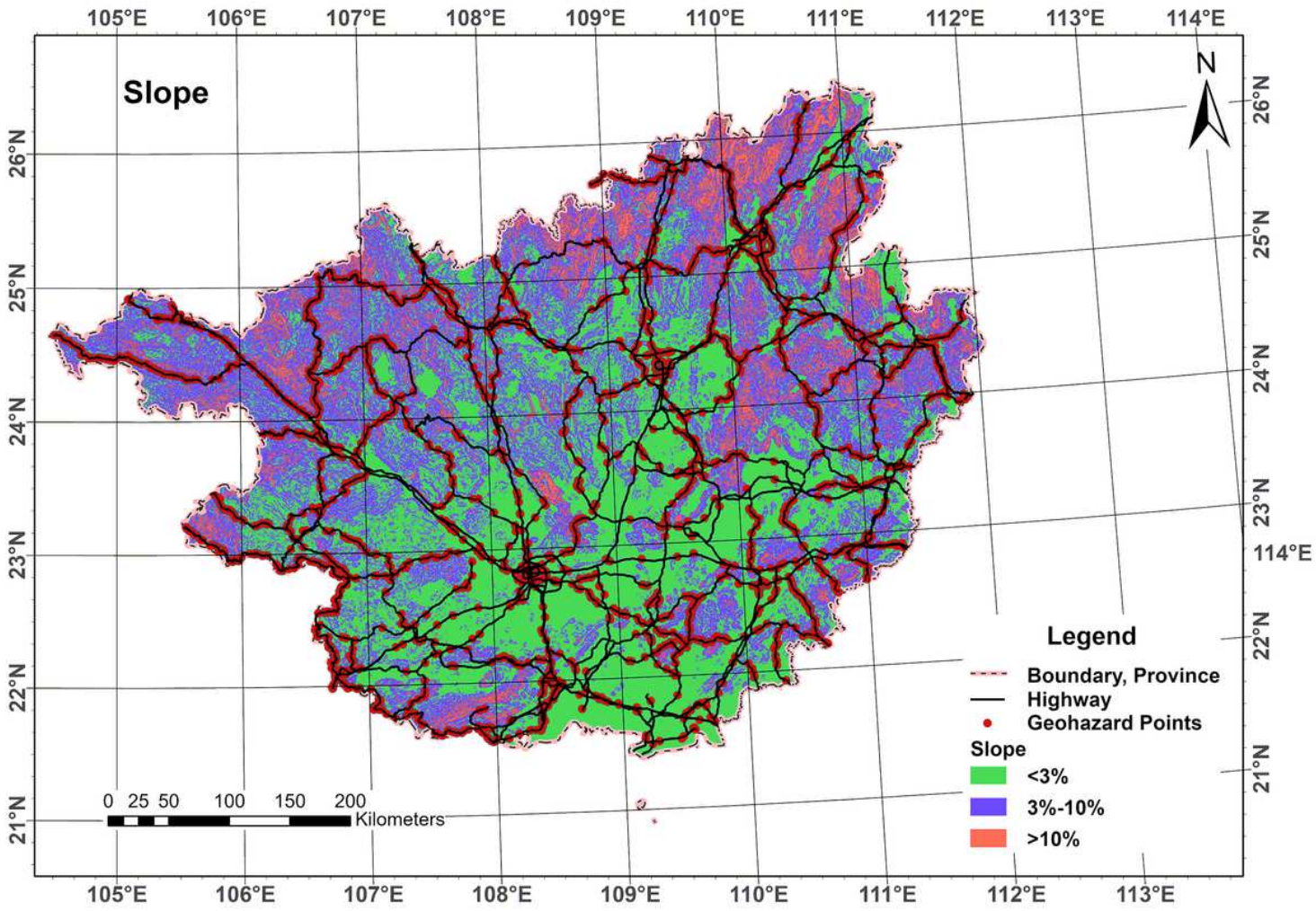

Figure 11

Slope distribution map

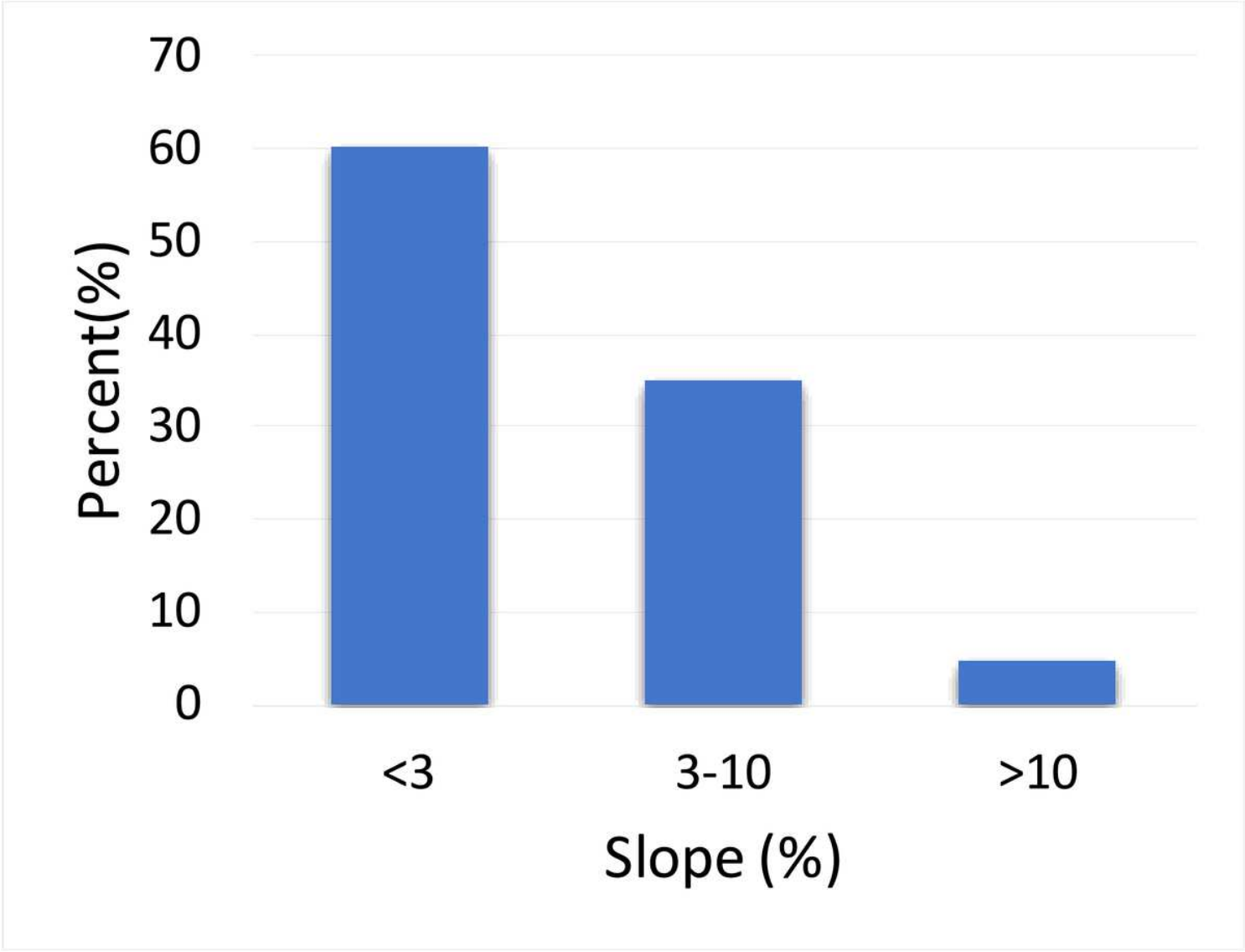

Figure 12

Relationship between slope and geohazards

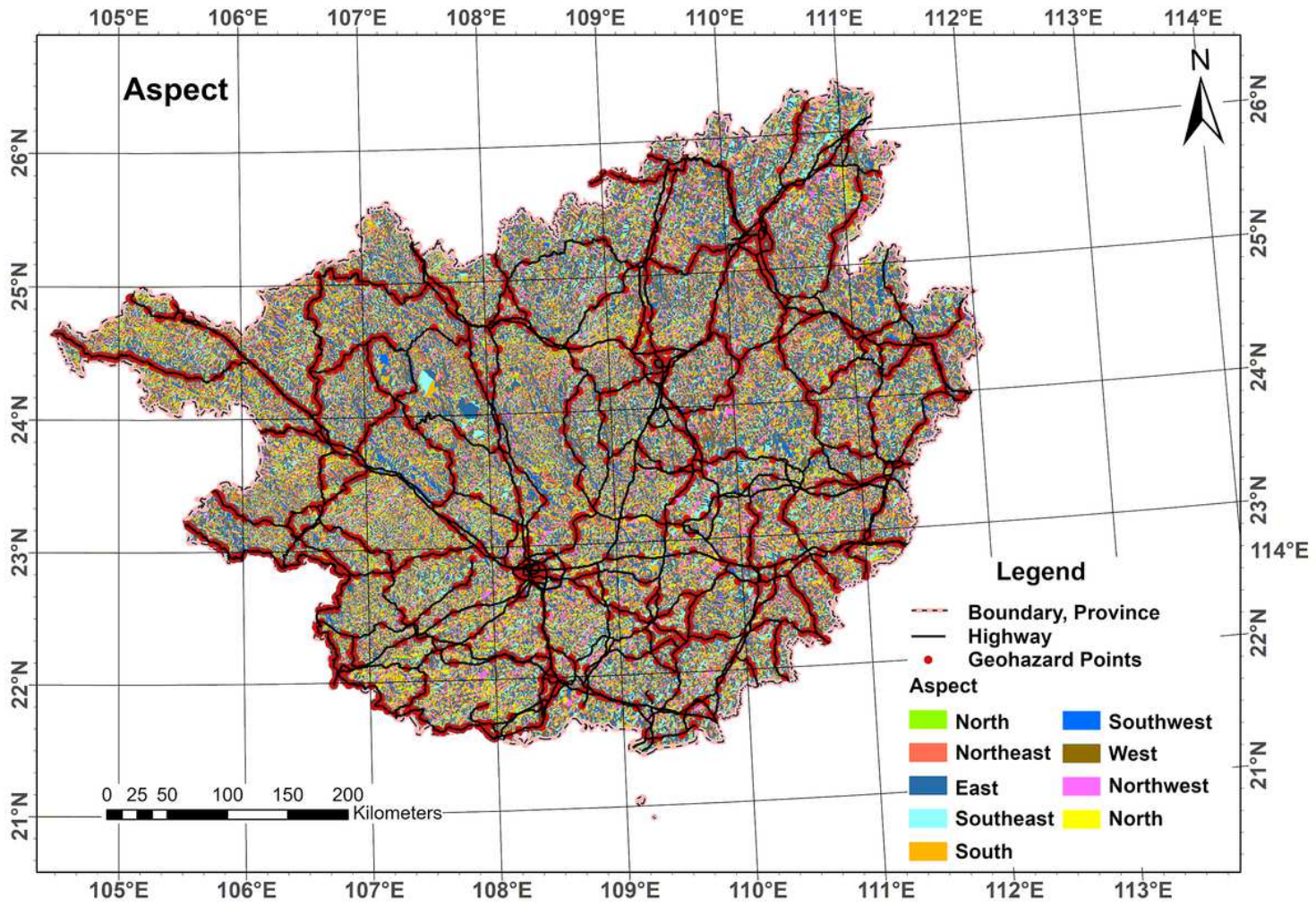

Figure 13

Aspect distribution map

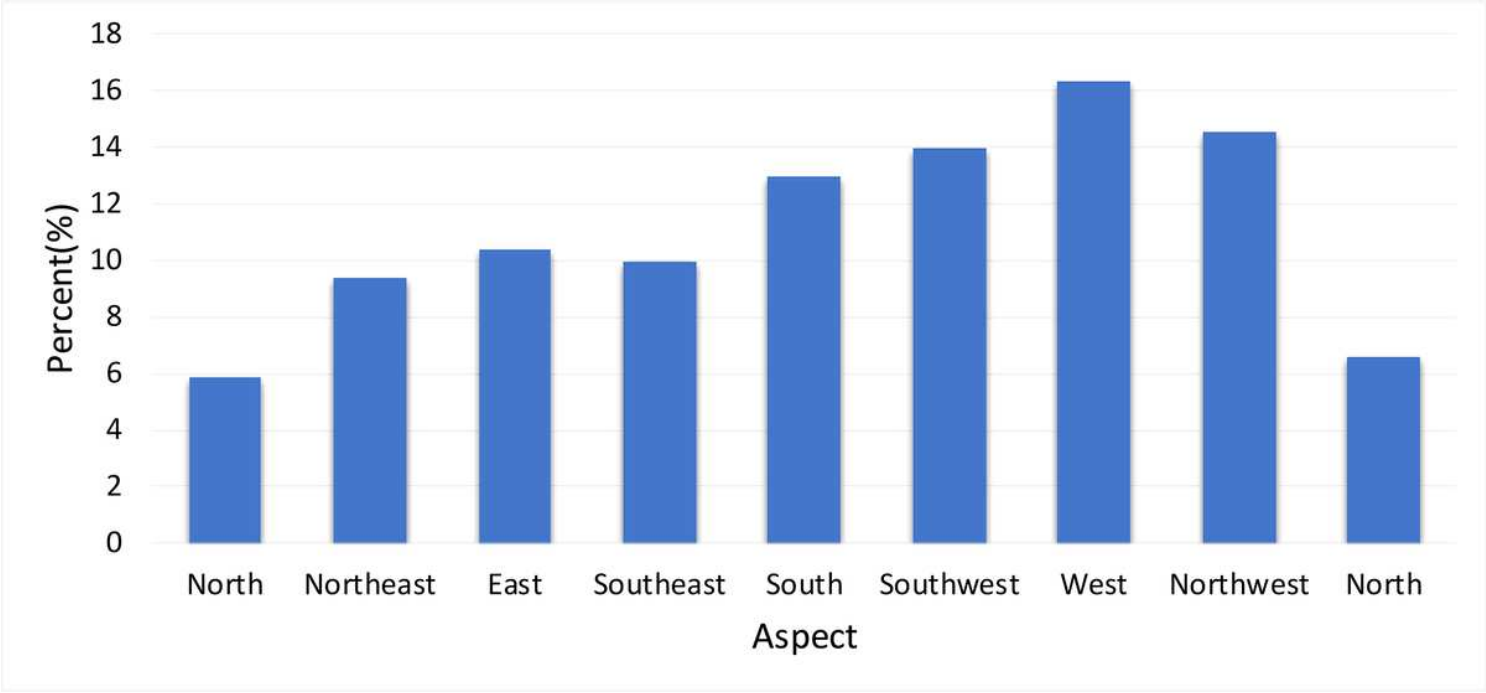

Figure 14

Relationship between aspect and geohazards

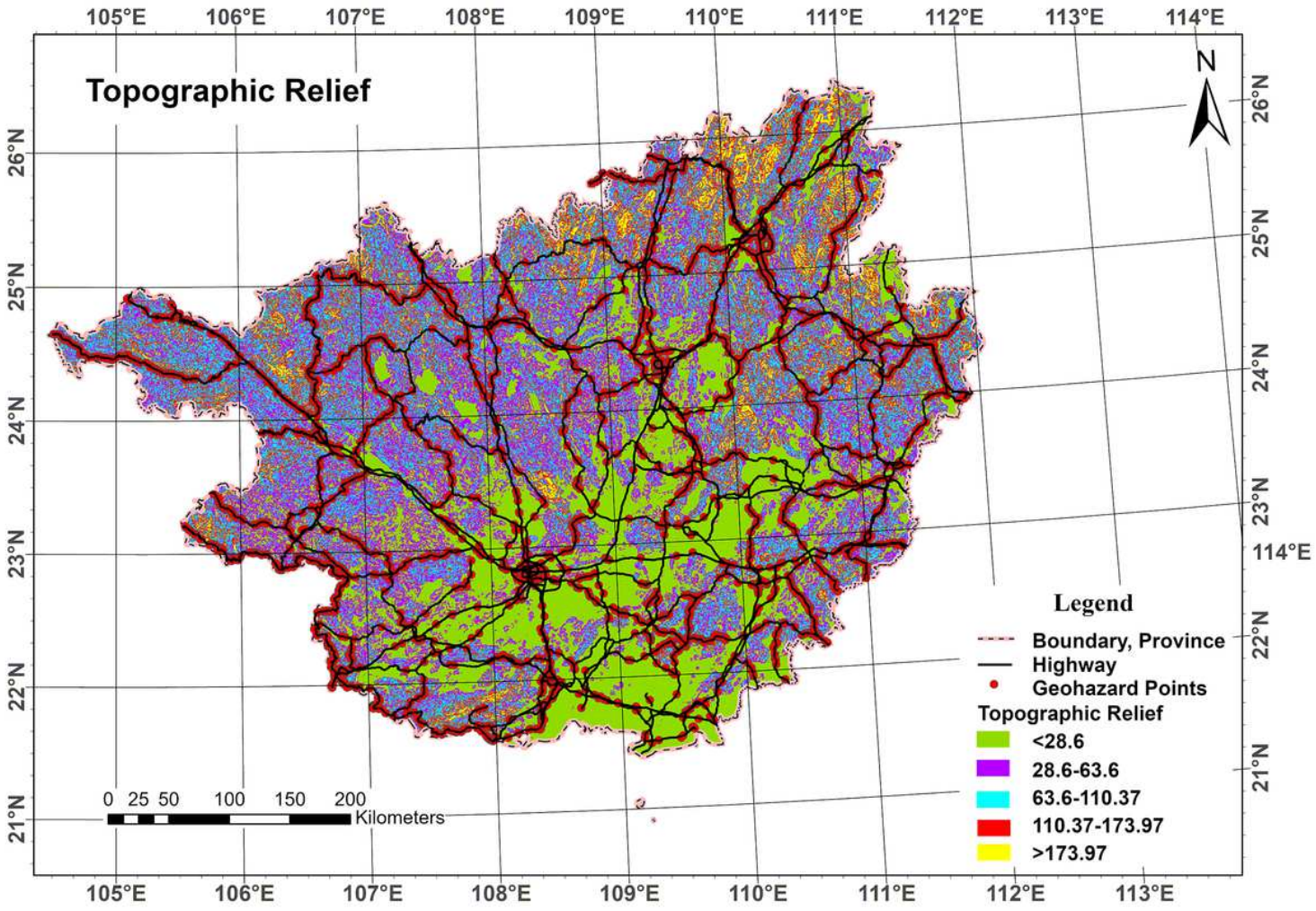

Figure 15

Topographic relief distribution map

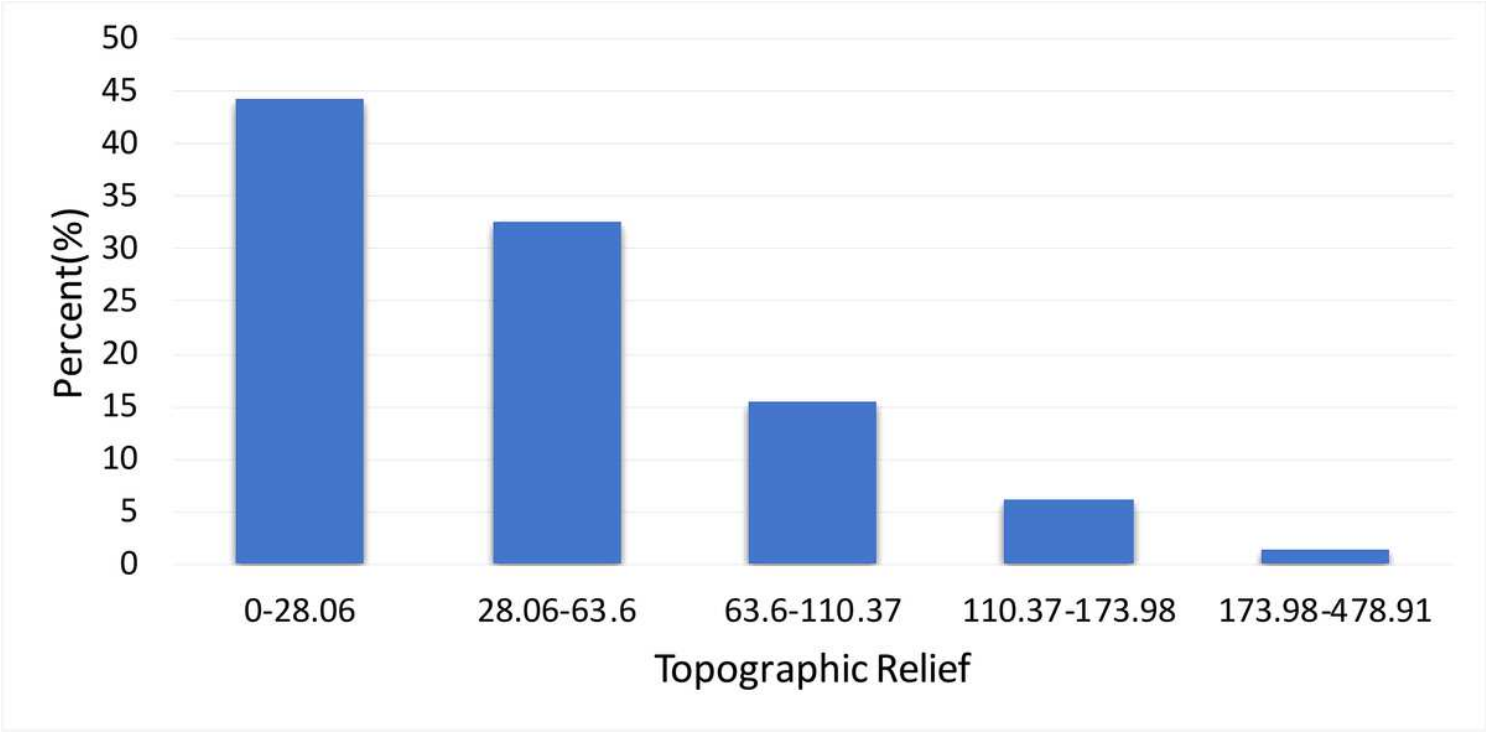

Figure 16

Relationship between topographic relief and geohazards

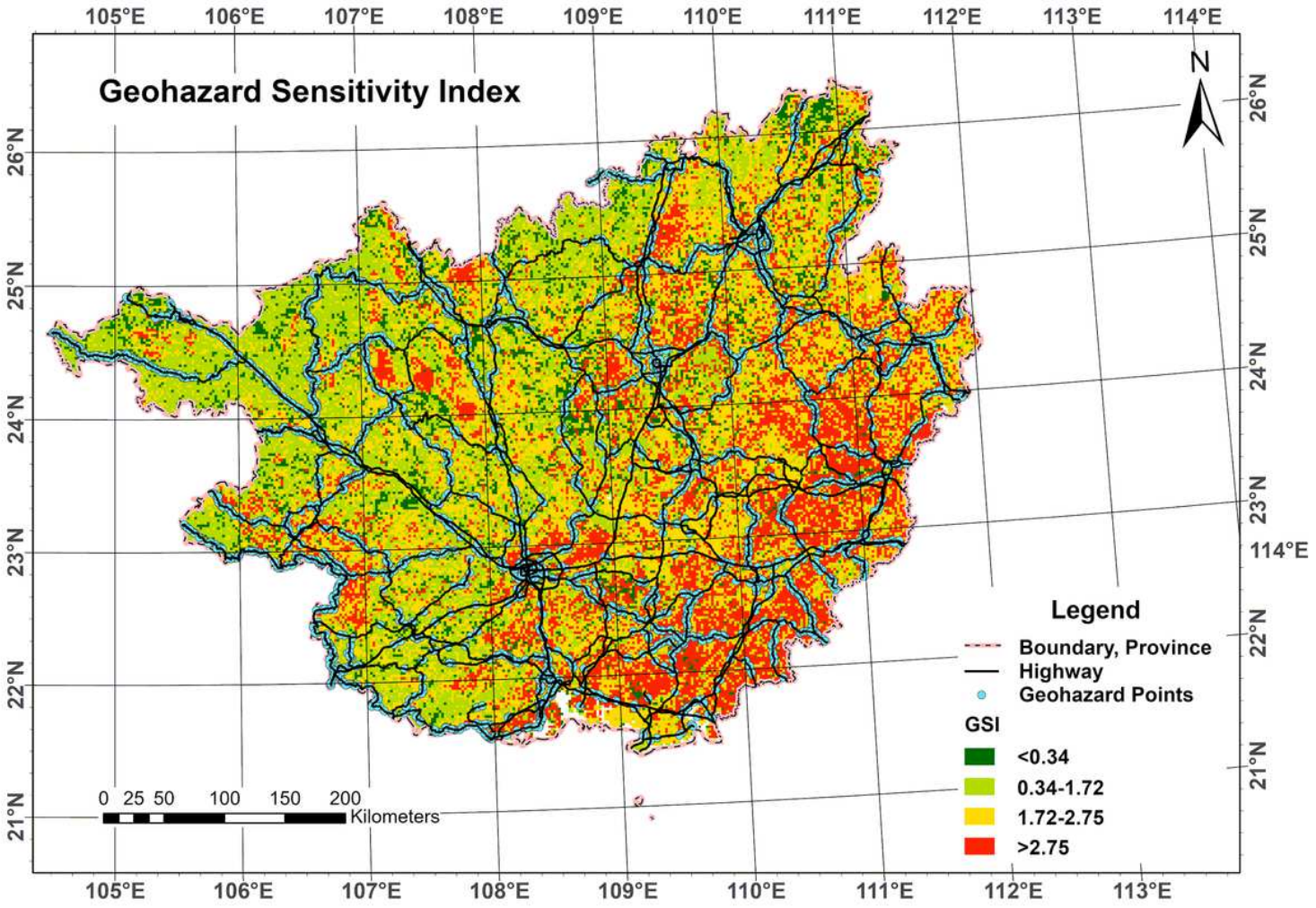

Figure 17

Map of geohazard sensitivity index along highways in Guangxi

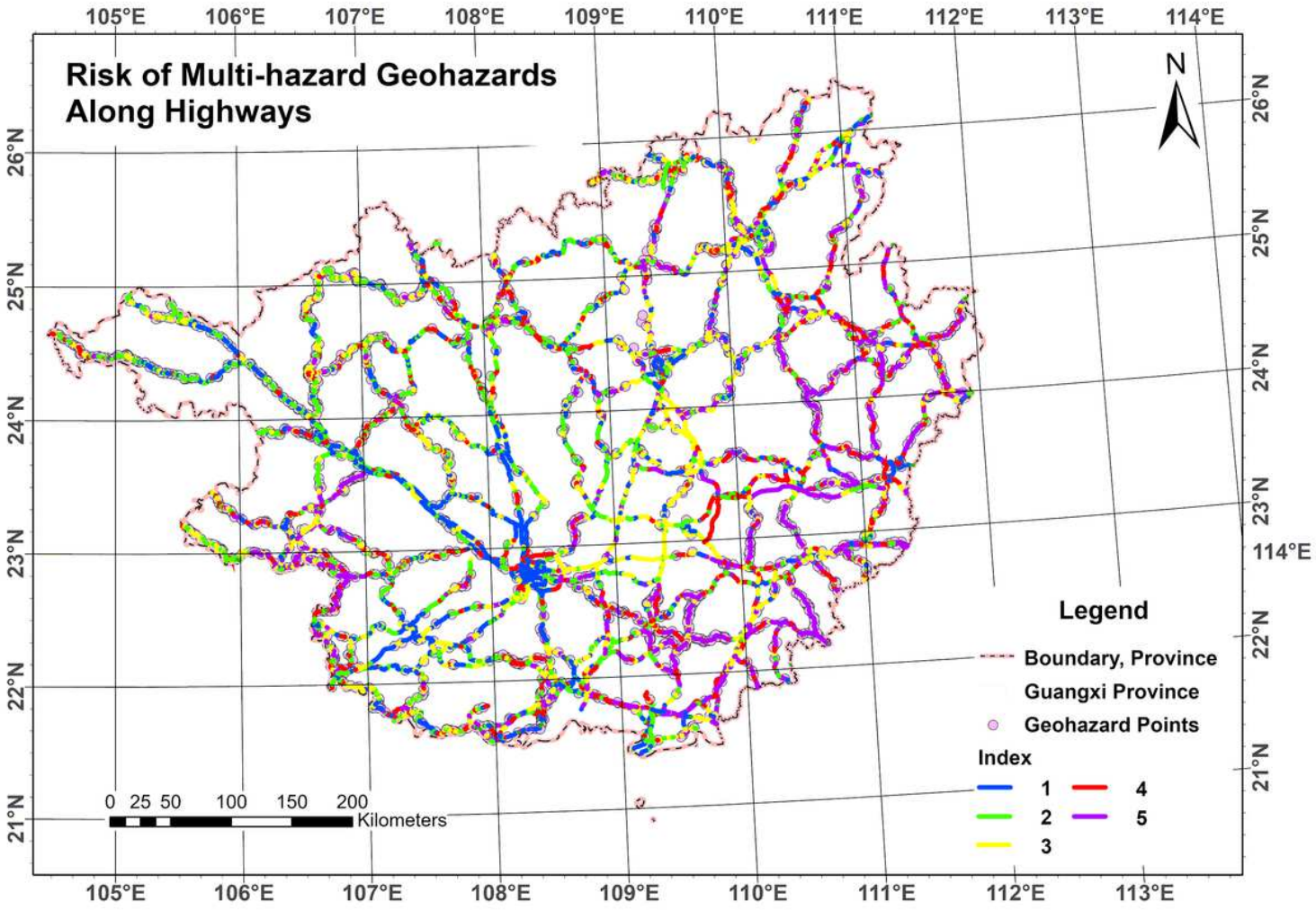

Figure 18

Geological hazard risk zoning map along highways in Guangxi Province

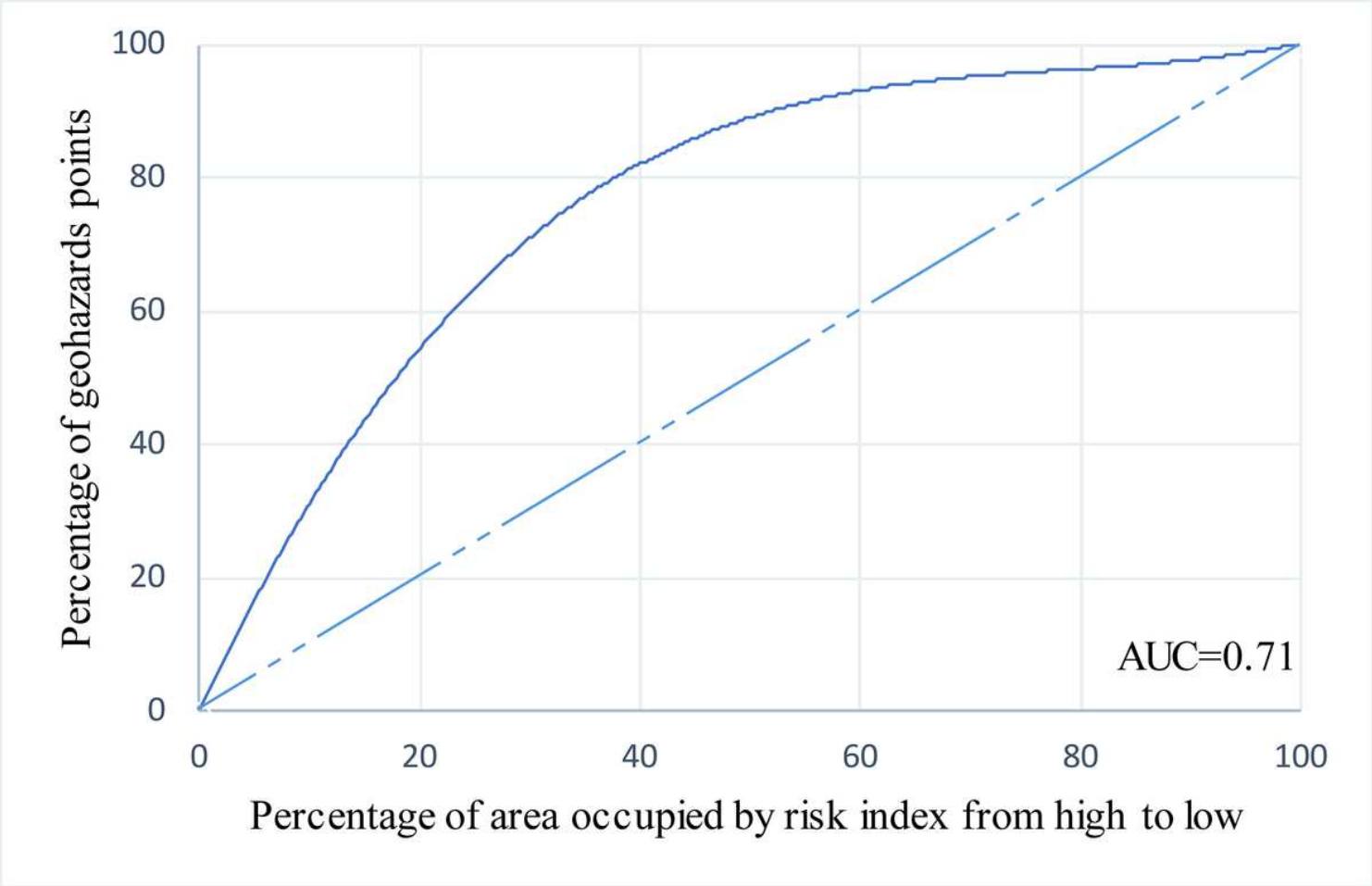

Figure 19

Map of receiver operating characteristic